Extremely high density of magnetic excitations at $T = 0$ in $YbCu_{5-x}Au_x$

I. Čurlík,[1] M. Giovannini,[2] J. G. Sereni,[3] M. Zapotoková,[1] S. Gabáni,[4] and M. Reiffers[1,4]

[1]*Faculty of Sciences, University of Prešov, 17 Novembra 1, SK 080 78 Prešov, Slovakia*

[2]*CNR-SPIN and Department of Chemistry, University of Genova I, 16146 Genova, Italy*

[3]*Low Temperature Division (CAB-CNEA), CONICET, 8400 S. C. de Bariloche, Argentina*

[4]*Institute of Experimental Physics SAS, Watsonova 47, SK 040 01 Košice, Slovakia*

(Received 21 August 2014; revised manuscript received 13 November 2014; published 5 December 2014)

Structural, magnetic, transport, and thermal properties of $YbCu_{5-x}Au_x$ alloys with Au concentration between $x = 0.4$ (at the stability limit of $AuBe_5$-type structure) and $x = 0.7$ are reported. The outstanding features of this system are (i) the constant and record high value of $C_m/T \approx 6.7$ J/mol K^2 below a characteristic temperature T^* (ranging between 150 mK and 350 mK), (ii) a power law of temperature dependence $C_m/T(T > T^*) = g/T^q$, with q ranging between 1.3 and 0.95 for decreasing x from 0.7 to 0.5, and (iii) an observation of incoherent electronic scattering in the resistivity at $T < 1$ K for $x \leqslant 0.6$ despite the fact that Yb magnetic atoms are placed in an ordered lattice. Geometric frustration, originating from the tetrahedral distribution of Yb atoms, appears to be responsible for the lack of magnetic order and the exotic behavior of this system.

DOI: 10.1103/PhysRevB.90.224409 PACS number(s): 71.28.+d, 75.30.−m, 75.50.−y

I. INTRODUCTION

The strong correlations between electrons in lanthanide- and actinide-based intermetallics give rise to a variety of physical phenomena originated in the hybridization of f states with the conduction band. The ground state formation in Ce, Yb, and U compounds is generally governed by the competition between intersite magnetic interactions RKKY, which favor magnetic order, and the local screening of magnetic moments induced by the Kondo effect [1–4]. Since both effects are driven by the exchange interaction (J_{ex}) between conduction and f electrons, the systems can be tuned from magnetic to nonmagnetic states (and vice versa) by nonthermal parameters (composition, pressure, magnetic field) [3–5]. By driving the phase boundary of the order transition to zero by means of these control parameters, the system may undergo a quantum phase transition at a quantum critical point (QCP) [6,7]. Around the critical region, low-energy collective excitations dominate the low-temperature physical properties and, as the temperature decreases, the density of these excitations increases. This is reflected in logarithmic or power-law temperature dependencies of their thermodynamic properties such as specific heat, magnetization, or thermal expansion, which are denoted as non-Fermi-liquid behaviors [8–10]. In addition to the suppression of magnetic order by Kondo effect, there is growing evidence that geometrical frustration may enhance quantum fluctuations with a consequent vanishing of magnetic order in favor of exotic ground states [11].

Heavy-fermion compounds which are tuned close to a QCP show high values of C_p/T for $T \to 0$, usually $\geqslant 1$ J/mol K^2. There is, however, a group of very heavy fermions showing nearly coincident record values $\approx$7 J/mol K^2 like YbPtBi and $YbCo_2Zn_{20}$, $\approx$6.5 J/mol K^2 for $PrAg_2In$, and $\approx$5.6 J/mol K^2 for $CeNi_9Ge_4$ [12–15]. A common feature of these compounds is a partial contribution of their first excited crystal field levels to their ground state (GS) properties, because their respective Kondo temperatures are comparable to the crystal field splitting (i.e., $T_K \approx \Delta_I$). For $CePd_3B_{0.5}$, where the GS is a pure Kramers doublet, a similar high value of $C_p/T(T \to 0) = 4.4$ J/mol K^2 was found [16], with the lowest characteristic temperature $T^* \approx 1$ K and reaching the full entropy $S_m = R \ln 2$ of the GS at $T \approx 4$ K [17]. Due to the scarce number of intermetallic compounds showing such large values of density of excitations at $T \to 0$, to recognize other exemplary systems with these peculiar characteristics is highly desirable, particularly among Yb-based compounds showing a pure Kramers GS doublet.

For such a purpose, new Yb compounds with magnetic transitions at very low temperature ($T_N \leqslant 1$ K), which can be tuned by alloying the ligand atoms, merit investigation. The $YbCu_{5-x}Au_x$ system is a proper candidate since it presents an extremely low Kondo temperature and it orders at $T_N < 1$ K [18,19]. This solid solution, crystallizing in the cubic $AuBe_5$-type structure, has recently received considerable attention due to the evolution of GS properties by Cu/Au substitution. The interest in this topic was initially triggered by the investigation on heavy-fermions of the family $YbCu_4T$ (T = Ag, Au), which crystallize in the cubic $MgCu_4Sn$ type (an ordered derivative of the $AuBe_5$ type). In particular, it was found that $YbCu_4Au$ orders magnetically below 1 K [20]. Later on, it was realized that YbCu4Au, like analogous members of the type $YbCu_4T$ (T = Ag, In) [21–23], is actually a point of crystallographic order of a $YbCu_{5-x}Au_x$ solid solution. Starting from the magnetically ordered $YbCu_4Au$, the substitution of Au by Cu (i.e., decreasing x) drives the system to the disappearance of the magnetic order [24]. On the stoichiometric limit, the nonmagnetic heavy fermion $YbCu_5$ (i.e., $x = 0$) could be prepared as cubic $AuBe_5$ crystal structure only at high pressure [21] or by melt spinning [25], while careful structural analysis of $YbCu_{5-x}Au_x$ solid solutions [26,27] has shown that homogeneous compounds with cubic $AuBe_5$-type structure can form as single phase at ambient pressure only for $x \geqslant 0.4$, questioning the previous findings on the composition of a possible QCP below $x = 0.4$ [28]. A transition temperature in the region close to the lower limit $x = 0.4$ has been determined just from the change in slope in the resistivity vs temperature dependence [28], whereas the measurements of heat capacity have been done only for $x \geqslant 0.8$ [18]. For $YbCu_{4.4}Au_{0.6}$ no evidence of a transition to a magnetically ordered phase was observed down to 20 mK

from recent measurements of magnetization, zero-field and longitudinal-field muon spin relaxations (μSR), and nuclear quadrupole resonance (NQR) [29]. Thus, it still remains an open question about the eventual existence of a QCP and its position on the concentration axis in the $YbCu_{5-x}Au_x$ system. With the aim to attain more information on the evolution of the ground state properties in this system, the present paper reports our investigation of the $YbCu_{5-x}Au_x$ solid solution in the region close to the lower Au concentration limit, through measurements of susceptibility above 2 K, resistivity and heat capacity down to lower temperature regions.

II. EXPERIMENTAL DETAILS

The polycrystalline samples of $YbCu_{5-x}Au_x$ ($x = 0.4,0.5,0.6,0.7$) have been prepared by weighting the stoichiometric amount of elements with the following nominal purity: Yb (99.9% mass), Cu (99.999% mass), and Au (99.99% mass). To avoid the loss of Yb with a high vapor pressure, the elements were enclosed in small tantalum crucibles and sealed by arc welding in argon atmosphere. The samples were then melted in an induction furnace, under a stream of pure argon. To ensure homogeneity during the melting, the crucibles were continuously shaking. The samples were then annealed in a resistance furnace at 700 °C for two weeks and finally quenched in cold water. The alloys were characterized by optical and electronic microscopy and by quantitative electron probe microanalysis (EPMA). The crystalline structure was examined by x-ray diffraction (XRD). Heat capacity measurements in the temperature range 0.4–300 K and in an applied magnetic field up to 9 T were performed with a PPMS device (Quantum Design) using the two-tau model of the relaxation method. For temperature range below 1 K down to 50 mK, a ^{3}He-^{4}He minidilution refrigerator was used. Electrical resistivity was measured also with the PPMS device using the 4-wire ac technique in the temperature range 0.4–300 K. Magnetic susceptibility (at excitation field 100 Oe) and magnetization were measured with an MPMS device (Quantum Design) in the temperature range 2–300 K and in an applied magnetic field up to 5 T.

III. EXPERIMENTAL RESULTS

All the alloys along the $YbCu_{5-x}Au_x$ ($x = 0.4,0.5,0.6,0.7$) section were single phase of cubic $AuBe_5$ structure type as determined from EMPA and XRD. Lattice parameters were evaluated by the least-squares method and their values are in accordance with those reported in Refs. [27,28] (see Ref. [30] for a comparison of these data). Since these compounds crystallize in a fcc lattice of the $AuBe_5$ structure type, the Yb magnetic atoms are located on a network of edge-sharing tetrahedra [30,31].

The temperature dependence of the inverse magnetic susceptibility $1/\chi(T)$ is displayed in Fig. 1. These results show the typical Curie-Weiss behavior for $T > 50$ K, with an effective magnetic moment $\mu_{\rm eff} \approx 4.3\mu_B$, close to the expected value for Yb^{3+} ions with a $J = 7/2$ spin-orbit ground state and in good agreement with those from Yoshimura *et al.* [28]. Below 50 K, the negative curvature indicates the effect of the thermal population reduction of the excited crystal electric field (CEF) levels. According to Lea, Leask, and Wolf (LLW) [32], the CEF in cubic symmetry splits the eightfold $J = 7/2$ ground state into two doublets (Γ_6 and Γ_7) and one quartet (Γ_8). Such a negative curvature in $1/\chi(T)$ reveals a reduction of $\mu_{\rm eff}$ due to a weaker intensity of the GS magnetic moment.

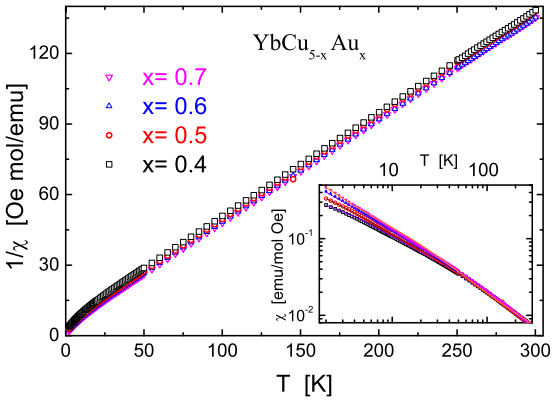

FIG. 1. (Color online) Temperature dependence of the inverse magnetic susceptibility $1/\chi(T)$ of $YbCu_{5-x}Au_x$ for $x = 0.4,0.5,0.6,0.7$ in a field $H = 50$ Oe. Inset: Magnetic susceptibility $\chi(T)$ in a double-logarithmic representation to show the variation of the low-temperature properties with Au concentration.

The contribution to the molecular field, manifested through the paramagnetic temperature (Θ_P), shows its concentration dependence with values between $\Theta_P = -10$ K (for $x = 0.7$) and -17 K (for $x = 0.4$). The negative Θ_P values, which indicate an antiferromagnetic (AFM) character of the magnetic interaction, are in good agreement with the literature [28]. The details of the low-temperature $\chi(T < 50$ K) results, included in the inset of Fig. 1, are discussed in Sec. IV.

The temperature dependencies of the electrical resistivity $\rho(T)$ of $YbCu_{5-x}Au_x$ for $x = 0.4,0.5,0.6,0.7$ are shown in Fig. 2. The measurements are compared with the $\rho(T)$

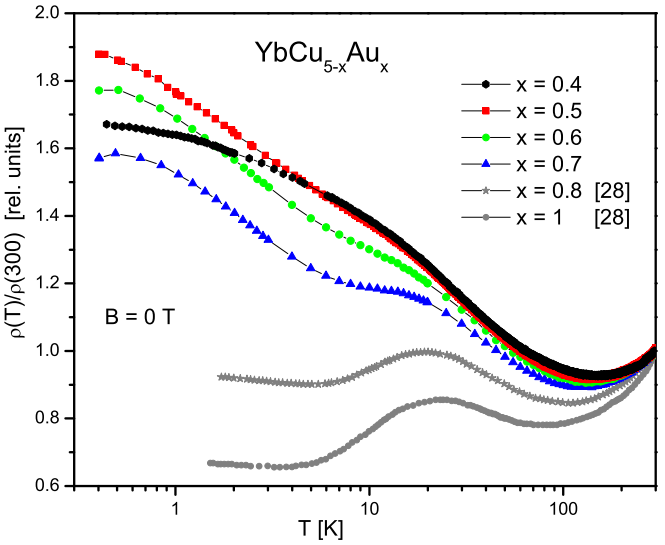

FIG. 2. (Color online) Normalized thermal dependence of electrical resistivity. Results from $YbCu_{5-x}Au_x$ alloys with $x = 0.4,0.5,0.6$, and 0.7 (this work), and $x = 0.8$ and 1 (see Ref. [28]).

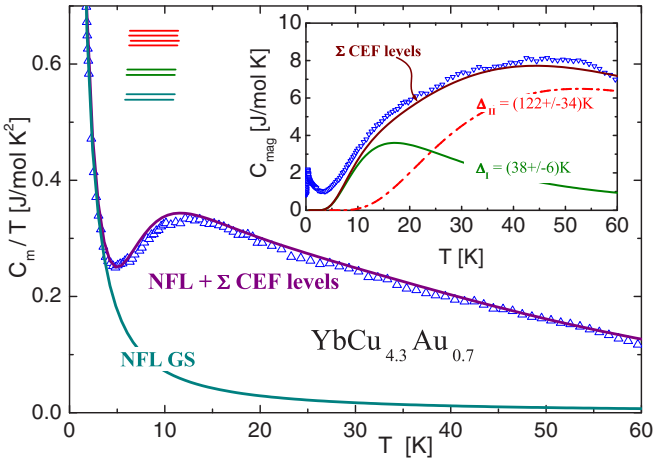

FIG. 3. (Color online) Magnetic specific heat divided by temperature for $YbCu_{4.3}Au_{0.7}$, showing the fitting curve with the NFL behavior of the (doublet) GS and the contribution of the excited CEF levels: a doublet at Δ_I and a quartet at Δ_{II}. Inset: Detail of the contribution from each excited CEF (see the text).

curves for $x = 0.8$ and 1 taken from the literature [28]. The high-temperature region (above 30 K) of $\rho(T)$ for all the samples is characterized by a nearly logarithmic increase with temperature decreasing, which is attributed to incoherent Kondo scattering related to the excited CEF levels. The broad maximum around 20 K is assigned to the position of the first crystal field level in the presence of Kondo interaction. However, marked differences exist between the magnetic ordered compound $YbCu_4Au$ ($x = 1$) and the other alloys. In fact, $YbCu_4Au$ exhibits typical Kondo lattice features with a clear onset of coherent scattering of the conduction electrons below about 20 K. On the contrary, the alloys with $x = 0.7$ and 0.6 are characterized by a progressive rise of the low temperature resistivity, with an incipient flattening of $\rho(T)$ below 1 K, which for sample $x = 0.4$ begins at $T \approx 10$ K likely due to the fact that this concentration is at the limit of the AB_5 structure stability [30]. These features clearly discard either the possibility of magnetic order or a Fermi-liquid GS formation as was previously proposed [29].

The specific heat of selected alloys was measured up to 60 K and the magnetic contribution (C_m) was obtained by subtracting the phonon contribution taken from the nonmagnetic isotypic compound YCu_4Au [33]. In Fig. 3 the temperature dependence for sample $YbCu_{4.3}Au_{0.7}$ is shown in a C_m/T representation. In this range of temperature, the excited CEF levels develop their respective temperature-dependent contributions. The figure inset displays the details of the proposed fitting curve, which includes the corresponding Schottky anomalies for the excited CEF levels, one doublet and one quartet. A proper fitting procedure, including the usual hybridization effects (V_{cf}) between conduction and $4f$ states acting on each exited level, requires complex calculation protocols [34]. Therefore in this case a very simple criterion to simulate the level broadening was applied. Each degenerated CEF level Γ_i, with respective degeneracies $\upsilon_i = 2$ or 4, was split into single Dirac levels equally distributed in energy around the nominal value (i.e., its barycenter) of the original multiplet. For applying this procedure the strength of the hybridization should be smaller than the CEF splitting (Δ_i), i.e., $V_{cf} \sim T_K < \Delta_i$.

The detailed fitting analysis was performed on sample $x = 0.7$ below $T = 60$ K (see Fig. 3). The calculations for the CEF level contribution is shown in the inset. The best description corresponds to two levels at ± 8 K from the center at $\Delta_I = 40$ K, and two doublets at ± 34 K from the center at $\Delta_{II} = 122$ K. Taking the respective distances to the center (at Δ_i) as representative of the hybridization strength of each multiplet, and consequently of their respective Kondo temperature, we obtain $T_K^I \sim 8$ K and $T_K^{II} \sim 32$ K. Due to the simplicity of this procedure, and the fact that CEF contribution is progressively overcome by the phonon contribution at this temperature range, the computed values have to be considered within $\pm 10\%$ of uncertainty.

These results can be tested by applying the Hanzawa criterion $T_K^h = (T_K \Delta_I ... \Delta_N)^{1/(N+1)}$ for the Kondo temperature scale evaluation in a CEF scenario (see Ref. [35]) as $T_K = (T_K^h)^{(N+1)}/(\Delta_I ... \Delta_N)$. For $N = 1$ (i.e., including only the first excited CEF level) one obtains $T_K = (T_K^I)^2/\Delta_I \approx 1.6$ K, and for $N = 3$ the Kondo temperature is $T_K = (T_K^{II})^4/(\Delta_I \Delta_{II}{}^2) = 1.7$ K (notice that the second excited state is a quartet). Similar values are obtained in Sec. IV from the analysis of thermal properties. Therefore, independently from the strict application of a particular model to our real system, we can anticipate that the scale of energy related to the Kondo effect is $T_K \leqslant 2$.

As can be seen in Fig. 3, the sum of these Schottky anomalies plus the contribution of the GS (to be discussed below) provides a proper description of the experimental results including an estimation of the hybridization effects on each excited CEF level. Specific heat measurements cannot distinguish between two levels of the same degeneracy, in this case between the doublets of $\upsilon = 2$, Γ_6, and Γ_7. According to LLW calculations, both Γ_6-Γ_7-Γ_8 and Γ_7-Γ_6-Γ_8 spectral distributions are possible [32]. In any case, the Γ_8 quartet (with $\upsilon = 4$) becomes unambiguously identified as the highest excited level. Previous neutron scattering studies performed on $YbCu_4Au$ report another CEF level spectrum, where the quartet Γ_8 is the first excited CEF level [36]. Such a pattern is not consistent with the present $C_m(T)$ results, because the maximum of the Schottky anomaly between the GS doublet and the quartet would exceed the measured values at $T = 0.42\Delta_I$. Nevertheless, the quasielastic linewidth ($\Gamma/2$) observed by neutron scattering is in good agreement with the T_K extracted from the fitting results shown in Fig. 3 since $\Gamma/2 \approx 8$ K at $T = 40$ K and $\Gamma/2 \approx 22$ K at $T = 124$ K. Within the main scope of this investigation, the relevant information extracted from this analysis is that the first excited CEF level practically does not contribute to the GS properties at low temperature, because $T_K(V_{cf}) \ll \Delta_I$. Thus, this system can be considered as the heaviest fermion system among reported materials with a well isolated doublet GS. Other mentioned Yb compounds with even higher $C_P/T(T \to 0)$ values, like those mentioned in the introduction, show more comparable values of T_K and Δ_I.

Low-temperature specific heat measurements are displayed in Fig. 4 as C_P/T vs T in a semilogarithmic scale for the studied $YbCu_{5-x}Au_x$ alloys with $x = 0.4, 0.5, 0.6, 0.7$. These

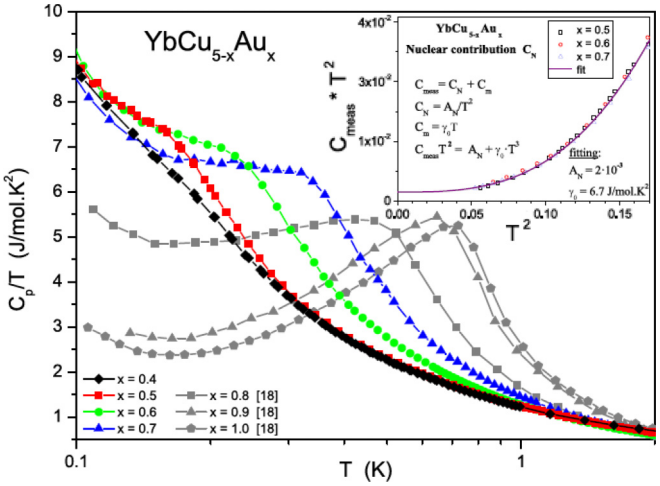

FIG. 4. (Color online) Heat capacity of $YbCu_{5-x}Au_x$ for $x = 0.4$, 0.5,0.6,0.7 (this work) and 0.8, 0.9, 1 (Ref. [18] plotted as C_p/T vs T in a logarithmic scale). Inset: The nuclear contribution fit of data in a $C_{\rm meas} \times T^2$ vs T^2 representation.

specific heat results are complemented in the figure with data from the literature [18] for $x = 0.8, 0.9, 1$. $YbCu_4Au$ exhibits a maximum in C_P/T around 0.7 K ascribed to the onset of long-range magnetic order. At low temperatures ($T < 0.4$ K), the increase of specific heat is attributed to the nuclear contribution (C_N). Since that contribution decreases as $C_N = A_N/T^2$, in order to make a quantitative evaluation we have plot the measured data using a $C_{\rm meas}T^2 = A_N + C_m(T)T^2$ temperature dependence. From the fits performed on the studied samples below $T = 0.4$ K we obtain that $A_N = 2 \times 10^{-3}$ and $C_m = \gamma_0 T$, with $\gamma_0 = 6.7$ J/mol K^2; see the inset in Fig. 4. For practical use, we label the experimental $C_m/T(T \to 0)$ value as the γ_0 factor; nevertheless it does not have to be identified with the standard Sommerfeld coefficient unless the low-energy excitations are proved to form a (heavy/narrow) band. Such does not seem to be the case for this system because of the incoherent electronic scattering observed for the alloys with $x \leqslant 0.7$.

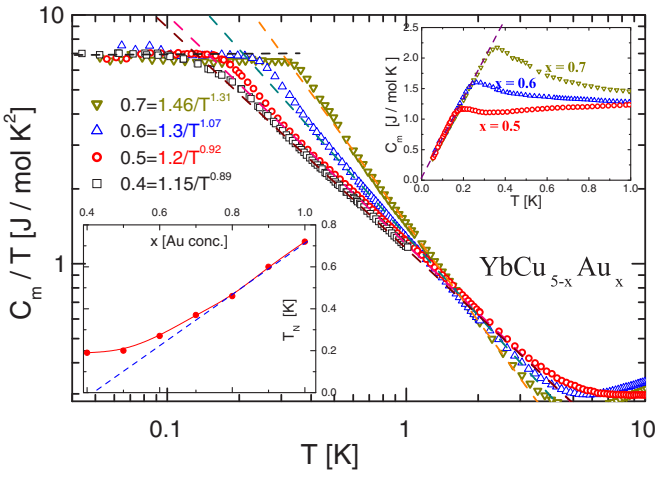

FIG. 5. (Color online) Very low temperature magnetic contribution to specific heat in a double-logarithmic representation (after subtraction of nuclear contribution). Dashed lines represent the respective power-law functions. Lower inset: Concentration dependence of $T_{\rm max}(x)$ split in two regions: as $T_N(x \geqslant 0.8)$ (blue squares) and $T^*(x \leqslant 0.7)$ (red circles). Upper inset: $C_m(T)$ representation showing the cusp at $T = T^*$.

As can be observed in Fig. 4, the shape of the C_m/T around the local maximum temperature $T_{\rm max}$ changes progressively from a well defined cusp for $x \geqslant 0.9$ alloys into a kink for $x \leqslant 0.7$. This modification in the shape of the maximum coincides with a change in the value of $C_m/T_{\rm max}$ from ~5.5 J/mol K^2 to ~6.7 J/mol K^2, indicating a change in the GS nature, which arises between $x = 0.9$ and $x = 0.7$. Within this range of concentration, γ_0 increases from 1.2 J/mol K^2 (at $x = 0.9$) [37] up to a saturation value of 6.7 J/mol K^2 for $x \leqslant 0.7$, whereas the $C_m/T \sim T$ dependence for $T < T_{\rm max}$ is progressively replaced by a constant $C_m/T = \gamma_0$ (see Fig. 5). One should notice that the significant tail of C_m/T above $T_{\rm max}$ shown in Fig. 4 is characteristic of a strong magnetic anisotropy or even of a two-dimensional system. This feature is analyzed in Sec. IV in the context of the thermal entropy dependence.

IV. DISCUSSION

In the inset of Fig. 1 the experimental results of the $\chi(T)$ dependencies are presented in a double-logarithmic representation. These results are well described by a standard Curie-Weiss law including the CEF splittings and the respective Van Vleck contributions:

$$\chi(T) = [(g_J\mu_B)^2/Z]\{\Sigma_i|\langle\Gamma_i\|\Gamma_i\rangle|^2\left[e^{-\Delta/kT}/k_B\left(T+\Theta_P^i\right)\right] + \Sigma_{ij}|\langle\Gamma_i\|\Gamma_j\rangle|^2[(e^{-\Delta_i/kT} - e^{-\Delta_j/kT})/\Delta_{ij}]\}, \quad (1)$$

where Z is the partition function, $\Gamma_i = \Gamma_6, \Gamma_7, \Gamma_8$, and Θ_p^i are the respective Curie-Weiss temperatures related to each molecular field contribution [38]. The CEF level splitting energies $\Delta_I = 40$ K and $\Delta_{II} = 124$ K, extracted from the high-temperature C_m measurements, were used as starting parameters (see Sec. III). For simplicity, the respective level widths are not taken into account. This produces a minor deviation from the experimental data at intermediate temperature, but not a low temperature because no broadening of the GS doublet is observed.

From these fittings the obtained effective paramagnetic moments are $\mu_{\rm eff}(GS) \approx (2.8 \pm 0.3)\mu_B$ and $\mu_{\rm eff}(\Delta_I) = (3.7 \pm 0.3)\mu_B$. These values are very close to the expected theoretical values for a Yb^{3+} ion with a Γ_7-Γ_6-Γ_8 spectral distribution [39] and converge to the $J = 7/2$ value ($4.54\mu_B$) at high temperatures. The Θ_P^i values for the excited CEF levels are those obtained from the analysis described in Sec. III. However, to properly fit the low-temperature curvature of the inverse susceptibility presented in Fig. 1, a ground state $\Theta_P^{\rm GS}$ parameter has to be evaluated. Differently from Θ_p^i values of the excited CEF levels, $\Theta_P^{\rm GS}$ shows a clear concentration dependence ranging between -0.7 K for $x = 0.7$ to -1.6 K for $x = 0.4$. These values indicate that any eventual Kondo screening is irrelevant for the GS properties within this range of Au concentration (i.e., $x \leqslant 0.7$). Notably, all the $\chi(T)$ results of these samples fit very well into the standard Curie-Weiss law [i.e., $\chi(T) \sim 1/(T + \Theta_P)$] with the only variation of $\Theta_P^{\rm GS}$, at variance from the $T^{-2/3}$ dependence reported in the literature [29].

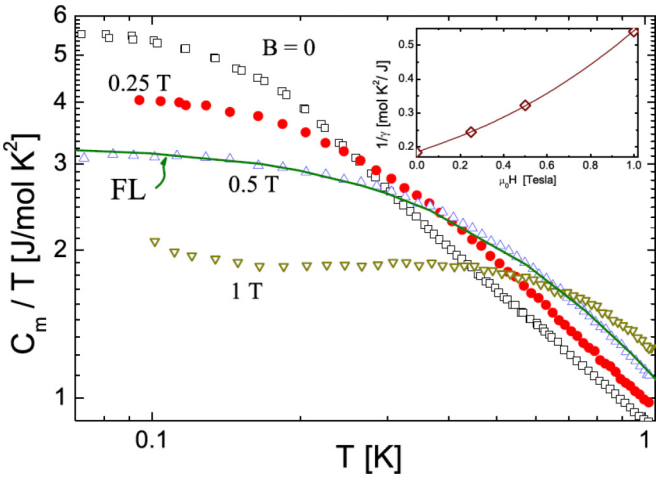

FIG. 6. (Color online) Effect of the magnetic field on the specific heat in sample with $x = 0.4$ in a double-logarithmic representation. Full curve represents a Fermi liquid thermal dependence. Inset: Inverse of γ_0 as a function of applied magnetic field.

Figure 5 shows the temperature dependencies of C_m/T for the $YbCu_{5-x}Au_x$ alloys with $x = 0.5, 0.6, 0.7$. For the sample with Au concentration $x = 0.4$ we observed reduced absolute value of C_m/T in the low temperatures; this dependence is presented in Fig. 6. For all the samples a constant $C_m/T = \gamma_0$ plateau below a characteristic temperature T^* appears, starting from $T^* \approx 0.35$ K for $x = 0.7$ to $T^* \approx 0.15$ K for $x = 0.4$ (see the lower inset in Fig. 5). The observed value $\gamma_0 \approx 6.7$ J/mol K^2 is comparable to the highest values reported from some other Yb-based compounds [12,40] with $\gamma_0 \approx 7.3$ J/mol K^2. Notably, in the $1 > x > 0.5$ range, the $\gamma_0(x)$ value increases with decreasing Au content (i.e., x) from values of $\approx$1 J/mol K^2 for $YbCu_4Au$ (i.e., $x = 1$) [37] up to $\gamma_0 \approx 6.7$ J/mol K^2 for $x = 0.7$, where it saturates. This variation is followed by the increase of the $C_m/T(x)$ maximum and the disappearance of the positive slope of C_m/T below T_{max}. These features suggest a progressive transformation of the GS nature, from a phase which develops some type of order parameter to some exotic nonordered phase with a constant density of excitations for $x \leqslant 0.7$. This is in agreement with previous results on $YbCu_{4.4}Au_{0.6}$, where no phase transition to a magnetically ordered state was detected down to 20 mK by μSR measurements. Instead, a dynamical muon relaxation driven by spin fluctuations and not by a static field distribution was found [29].

The low-temperature plateau of C_m/T ends in a kink at $T = T^*$, above which it drops down. A detail of the $C_m(T)$ dependence around T^* is presented in the upper inset of Fig. 5. Notably, no $C_m(T)$ jump occurs at T^*, rather a cusp related to a strong change of the $\partial C_m/\partial T$ derivative. Similar features are observed in other Ce and Yb compounds also showing divergent power-law dependencies in $C_m(T)/T$ at $T > T^*$ [41]. Because of the clear change in the GS properties between $x = 0.8$ and 0.7, we label the temperature of the maximum of $C_m(T)$ as T_N on the region showing some magnetic order and as T^* for $x \leqslant 0.7$, where no evidence of magnetic order is detected. In this concentration region the mentioned plateau of C_m/T is followed above $T = T^*$ by a power law $C_m/T = g/T^q$ dependence, with g ranging between 1.43 and 1.22 J/mol K^{1+q} and q between 1.3 and 0.95 for decreasing x from 0.7 to 0.5. This temperature dependence of C_m/T also changes for $x \geqslant 0.8$ as a further confirmation of the intrinsic transformation of the GS nature. In the inset of Fig. 5, the phase boundary between the quasi-paramagnetic phase, where $C_m/T(T)$ follows a power law, and the GS phase is presented.

At variance with the reported interpretation of resistivity measurements [28], we claim that this system shows a continuous transformation between $x = 0.9$ and 0.7, with a possible mixture of two components suggested by the progressive increase of $\gamma_0(x)$. The temperature dependence of the electrical resistivity behaves accordingly, because no kinks in $\rho(T)$ are observed. Instead $T_N(x)$ is defined by the onset of coherence in the scattering of the conduction electrons with the magnetic lattice [28]. This effect of coherence practically disappears for $x \leqslant 0.7$ where $\rho(T)$ increases continuously by cooling, indicating the presence of incoherent scattering like in a single-impurity behavior (see Fig. 2). This phenomenology was also observed in the very heavy fermion systems ($\gamma_0 >$ 4 J/mol K^2) $CePd_3B_{0.6}$ [42] and $CeNi_9Ge_4$ [15], suggesting that a very high density of excitations does not imply the formation of an electronic band with coherent character.

As shown in the lower inset of Fig. 5, the concentration dependence of $T_N(x)$, defined in the range $1 \geqslant x \geqslant 0.8$ by the cusp in C_m/T, extrapolates to zero around $x = 0.5$. However, for $x \leqslant 0.7$ the temperature of the kink in C_m/T at $T^*(x)$ tends to saturate to a finite value ($T^* \approx 0.1$ K) as x decreases. This change in the concentration dependence between T_N and T^* coincides with the changes mentioned before in the $C_m/T(T)$ properties. The presence of a plateau is an unusual temperature dependence, only observed in a few heavy fermions showing the upper limit γ_0 values [43]. The question arises as to whether this peculiar feature is related to the extremely high values of $C_m/T(T)$ reached by the divergent power-law thermal dependence above T^*. It is evident that a continuous diverging trend below T^* would exceed the entropy of a doublet GS (i.e., $R \ln 2$). The $R \ln 2$ constraint for the twofold-degenerated GS implies that very high γ_0 values correspond to a very low energy scale or characteristic temperature. This condition excludes the T_K values of $\approx$10 K proposed in the literature [28].

These peculiar spectroscopic and thermodynamic results, including the observed dynamical spin susceptibility features on $YbCu_{4.4}Au_{0.6}$ [29], converge into the phenomenology of a frustrated magnetic system, in coincidence with the fact that no magnetic order is observed down to the millikelvin range of temperature despite the robust μ_{eff} values of Yb atoms. In fact, this structural configuration realizes the optimal conditions for a three-dimensional frustration because, as already mentioned in Sec. III, in the $AuBe_5$-type structure the magnetic Yb atoms are located on a network of edge-sharing tetrahedra. Further evidence for such a scenario is currently given by the empirical frustration parameter $f = |\Theta_P|/T_N$ [44] that for $0.7 \geqslant x \geqslant 0.4$ alloys rises from $\approx$1.9 up to $\approx$8.4. Although part of this ratio can be attributed to CEF effects, its significant increase with concentration cannot be explained by CEF energy level variation. An illustrative comparison can be done with the isotypic compound $GdCu_4In$ (Ref. [31]) and the Cd-doped

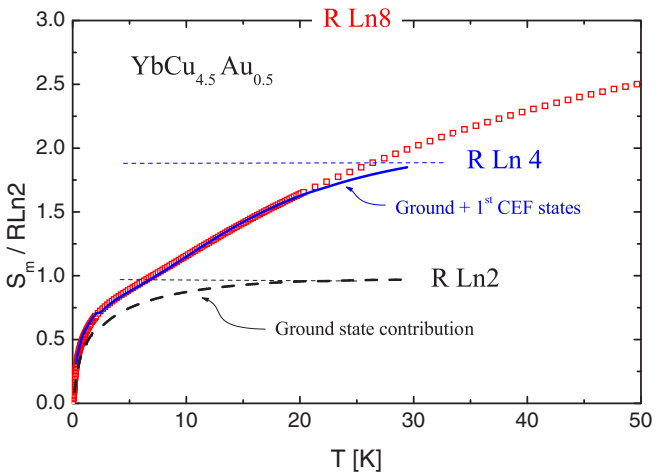

FIG. 7. (Color online) Temperature variation of the entropy of $YbCu_{4.5}Au_{0.5}$ below 60 K. Straight lines are references for the entropy of the excited CEF levels. Lower dashed curve represents the entropy of the GS, while the upper curve indicates the sum of the ground and the first CEF doublet, both computed from the thermal dependencies shown in Fig. 5.

alloys [45]. In this case, In substitution by Cd enhances next-nearest-neighbor (NNN) magnetic interactions allowing them to compete with nearest-neighbor (NN) interactions. As a consequence a relaxation of the frustration conditions occurs [31]. In the case of $YbCu_{5-x}Au_x$, Au and Cu atoms are isoelectronic, but their different atomic size introduces some atomic disorder. Although the increase of incoherent scattering observed by decreasing x may be partially explained by a growing atomic disorder, the mentioned NQR and μSR studies in $YbCu_{4.4}Au_{0.6}$ [29] reveal a dynamic character of spin susceptibility. Such a behavior cannot be attributed to static atomic disorder only, but also to frustration effects. Furthermore, the unusual appearance of a plateau in C_m/T below T^* for $x \leqslant 0.7$ indicates that some microscopic mechanism inhibits the formation of short-range order.

A further test of this scenario can be performed by studying the effect of applied magnetic field, since above a threshold value one may expect a spin fluctuation quenching. In Fig. 6, the effect of magnetic field on the specific heat on a sample with $x = 0.4$ is shown. Applying magnetic field reduces progressively the density of low-energy excitations, in accordance with the nuclear spin relaxation rates results [29]. However, the observed $1/\gamma_0$ dependence with H is linear for $\mu_0 H < 0.5$ T (see inset of Fig. 6), which is not in line with the conclusion that a Fermi liquid (FL) state is induced by magnetic field. In fact, in such a case a $1/\gamma_0$ vs H^2 dependence is predicted [46]. It is only under an applied field of 0.5 T that a FL thermal dependence is reached for the specific heat, as depicted by the full curve in Fig. 6. Therefore, these alloys behave as a non-FL in agreement with the observed power-law thermal dependence above $T = T^*$. Nevertheless, the spin fluctuation that control the GS properties are dumped by a field of ≈0.5 T. Notice that the energy $\mu_B H$ associated with an applied magnetic field of 0.5 T compares with the thermal energy $k_B T^*$.

In Fig. 7 the thermal variation of the magnetic entropy (S_m) of $YbCu_{4.5}Au_{0.5}$ below 50 K is presented. $S_m(T)$ shows a clear tendency to reach the total value of $R \ln 8$ expected for a $J = 7/2$ Hund's rule ground state above the temperature range of our measurements. The $R \ln 2$ value corresponding to a doublet GS is reached at $T \approx 7$ K, which indicates that only a doublet is involved in the GS properties according to the upturn of $C_m/T(T)$ around 6 K (see Fig. 3) where the first excited CEF doublet (at $\Delta_1 \approx 40$ K) starts to contribute to the specific heat. In Fig. 7, the lower (black) dashed curve represents the entropy of the GS, while the upper (blue) curve indicates the sum of the ground and the first CEF doublets, both computed from the temperature dependencies shown in Fig. 3. From the lower curve one can estimate that at $T \approx 7$ K the GS entropy accounts for about 80% of the total computed entropy. In order to characterize the low-temperature behavior of GS from entropy, one can evaluate the scale of energy T_0 applying the criteria used for Kondo impurities proposed by Desgranges and Schotte [47]. This criteria is valid for a GS doublet within the single-ion Kondo model: (i) $T_0 = (\pi R/3)/\gamma_0$ with a $\gamma_0 = 6.7$ J/mol K^2 value; this gives a $T_0 \approx 1.2$ K; and (ii) the temperature at which $S_m = 2/3R \ln 2$ (see Fig. 7) corresponds to $T_0 = 1.6$ K. Both values are in very good agreement with those obtained previously from the analysis on the high-temperature specific heat (Sec. III). These Kondo temperature values are notably small in comparison with those observed in other Yb- and Ce-based intermetallic compounds. The present scenario can be understood by the vicinity of these alloys to a quantum critical region where there is a possibility for a Kondo breakdown as was proposed some years ago [48]. The number of degrees of freedom of a doublet GS is fixed (cf. total $S_m = R \ln 2$) from the basic thermodynamic constraint. Therefore, one can infer that to very high γ_0 values corresponds the very small characteristic scales of energy obtained.

V. CONCLUSION

In this work, a systematic investigation on the $YbCu_{5-x}Au_x$ ($x = 0.4, 0.5, 0.6, 0.7$) system focusing on the record high value of $C_m/T(T \to 0) \approx 7$ J/mol K^2 is presented. Although such a value is comparable with a few previous compounds reported in the literature, in this case it corresponds to a well isolated Kramers doublet ground state as proved by high-temperature specific heat analysis. For all the samples prepared in this work, below a characteristic temperature T^* a plateau in C_m/T appears up to the lowest temperatures. It reaches the same value of around 7 J/mol K^2 for all the compounds with $0.5 < x < 0.7$. In fact, this high γ_0 value, corresponding to low temperature and high density of excitations, appears as an empirical upper limit. Such a limit is imposed by the amount of the available degrees of freedom fixed by $S_m = R \ln 2$. Above a characteristic temperature T^*, the $C_m/T(T)$ plateau transforms into a power-law temperature dependence. The apparent contradiction between the incoherent electronic scattering observed in the resistivity at $T < 1$ K for $x \leqslant 0.6$ despite the fact that Yb magnetic atoms are placed in a lattice is explained by magnetic frustration. This originates from the tetrahedral distribution of Yb atoms located in the 4*a* sites of the $AuBe_5$ structure type.

ACKNOWLEDGMENTS

This work was supported by the project VEGA 2/0070/12 and 2/0106/13, CFNT MVEP - the Center of Excellence of the Slovak Academy of Sciences, and the EU ERDF-ITMS26220120047 and ITMS26220120005. The liquid nitrogen for the experiment was sponsored by the US Steel Kosice, s.r.o. M.G. and J.S. acknowledge the VI Executive Program of Scientific and Technological Cooperation between Italy and Argentina 2014-2016, the FONCyT (Project No. PICT 1060-2010), and UNCuyo support (Project No. 06/C457).

[1] G. R. Stewart, Rev. Mod. Phys. **56**, 755 (1984).
[2] N. Grewe and F. Steglich, *Handbook of Physics and Chemistry of Rare Earths* (Elsevier, Amsterdam, 1990).
[3] E. Bauer, Adv. Phys. **40**, 417 (1991).
[4] J. G. Sereni, J. Phys. Soc. Jpn. **67**, 1767 (1998).
[5] M. Giovannini, H. Michor, E. Bauer, G. Hilscher, P. Rogl, T. Bonelli, F. Fauth, P. Fischer, T. Herrmannsdorfer, L. Keller, W. Sikora, A. Saccone, and R. Ferro, Phys. Rev. B **61**, 4044 (2000).
[6] H. von Löhneysen, A. Rosch, M. Vojta, and P. Wölfle, Rev. Mod. Phys. **79**, 1015 (2007).
[7] T. Muramatsu, T. Kanemasa, T. Kagayama, K. Shimizu, Y. Aoki, H. Sato, M. Giovannini, P. Bonville, V. Zlatic, I. Aviani, R. Khasanov, C. Rusu, A. Amato, K. Mydeen, M. Nicklas, H. Michor, and E. Bauer, Phys. Rev. B **83**, 180404(R) (2011).
[8] G. Steward, Rev. Mod. Phys. **73**, 797 (2001).
[9] R. Kuchler, N. Oeschler, P. Gegenwart, T. Cichorek, K. Neumaier, O. Tegus, C. Geibel, J. A. Mydosh, F. Steglich, L. Zhu, and Q. Si, Phys. Rev. Lett. **91**, 066405 (2003).
[10] E. Bauer, G. Hilscher, H. Michor, C. Paul, Y. Aoki, H. Sato, D. T. Adroja, J. G. Park, P. Bonville, C. Godart, J. Sereni, M. Giovannini, and A. Saccone, J. Phys.: Condens. Matter **17**, S999 (2005).
[11] M. S. Kim and M. C. Aronson, Phys. Rev. Lett. **110**, 017201 (2013).
[12] Z. Fisk, P. C. Canfield, W. P. Beyermann, J. D. Thompson, M. F. Hundley, H. R. Ott, E. Felder, M. B. Maple, M. A. Lopezdela Torre, P. Visani, and C. L. Seaman, Phys. Rev. Lett. **67**, 3310 (1991).
[13] T. Takeuchi *et al.*, J. Phys.: Conf. Ser. **273**, 012059 (2011).
[14] A. Yatskar, W. P. Beyermann, R. Movshovich, and P. C. Canfield, Phys. Rev. Lett. **77**, 3637 (1996).
[15] U. Killer, E. W. Scheidt, G. Eickerling, H. Michor, J. Sereni, T. Pruschke, and S. Kehrein, Phys. Rev. Lett. **93**, 216404 (2004).
[16] I. Zeiringer, J. G. Sereni, M. G. Berisso, K. Yubuta, P. Rogl, A. Grytsiv, and E. Bauer, Mater. Res. Express **1**, 016101 (2014).
[17] J. G. Sereni, G. Schmerber, and J. P. Kappler, IEEE Trans. Magn. **49**, 4647 (2013).
[18] M. Galli, E. Bauer, St. Berger, Ch. Dusek, M. Della Mea, H. Michor, D. Kaczorowski, E. W. Scheidt, and F. Marabelli, Physica B **312–313**, 489 (2002).
[19] E. Bauer *et al.*, Phys. Rev. B **60**, 1238 (1999).
[20] C. Rossel, K. N. Yang, M. B. Maple, Z. Fisk, E. Zirngiebl, and J. D. Thompson, Phys. Rev. B **35**, 1914 (1987).
[21] K. Yoshimura, N. Tsujii, J. He, M. Kato, K. Kosuge, H. Michor, K. Kreiner, G. Hilscher, and T. Goto, J. Alloys Compd. **262–263**, 118 (1997).
[22] H. Michor, K. Kreiner, N. Tsuji, K. Yoshimura, K. Kosuge, and G. Hilscher, Physica B **319**, 277 (2002).
[23] J. He, N. Tsujii, K. Yoshimura, K. Kosuge, and T. Goto, J. Phys. Soc. Jpn. **66**, 2481 (1997).
[24] M. Giovannini, A. Saccone, St. Muller, H. Michor, and E. Bauer, J. Phys: Condens. Matter **17**, S877 (2005).
[25] M. Reiffers, B. Idzikowski, J. Sebek, E. Santava, S. Ilkovic, and G. Pristas, Physica B **378–380**, 738 (2006).
[26] P. Carretta, M. Giovannini, M. Horvatic, N. Papinutto, and A. Rigamonti, Phys. Rev. B **68**, 220404(R) (2003).
[27] M. Giovannini, R. Pasero, S. De Negri, and A. Saccone, Intermetallics **16**, 399 (2008).
[28] K. Yoshimura, T. Kawabata, N. Sato, N. Tsujii, T. Terashima, C. Terakura, G. Kido, and K. Kosuge, J. Alloys Compd. **317–318**, 465 (2001).
[29] P. Carretta, R. Pasero, M. Giovannini, and C. Baines, Phys. Rev. B **79**, 020401(R) (2009).
[30] M. Giovannini, I. Čurlík, J. G. Sereni, F. Gastaldo, S. Gabáni, and M. Reiffers, [J. Alloys Compd. (to be published) (2014)].
[31] V. Fritsch, J. D. Thompson, and J. L. Sarrao, Phys. Rev. B **71**, 132401 (2005).
[32] K. R. Lea, M. J. Leask, and W. P. Wolf, J. Phys. Chem. Solids **23**, 1381 (1962).
[33] I. Curlik, Ph.D. thesis, Pavol Jozef Šafárik University, Košice, Slovakia, 2012.
[34] M. A. Romero, A. A. Aligia, G. L. Nieva, and J. G. Sereni, J. Phys.: Condens. Matter **26**, 025602 (2014).
[35] K. Hanzawa, K. Yamada, and K. Yosida, J. Magn. Magn. Matter **47–48**, 357 (1985).
[36] A. Severing, A. P. Murani, J. D. Thompson, Z. Fisk, and C.-K. Loong, Phys. Rev. B **41**, 1739 (1990).
[37] E. Bauer (private communication).
[38] H. Lueken, W. Brüggemann, W. Bronger, and J. Fleischhauer, J. Less Common Metals **65**, 79 (1979).
[39] R. J. Birgeneau, J. Phys. Chem. Solids **33**, 59 (1972).
[40] M. S. Torikachvili, S. Jia, E. D. Mun, S. T. Hannahs, R. C. Black, W. K. Neils, D. Martien, S. L. Bud'ko, and P. C. Canfield, Proc. Natl. Acad. Sci. USA **104**, 9960 (2007).
[41] J. G. Sereni, J. Low Temp. Phys. doi:10.1007/s10909-014-1228-z (2014).
[42] G. Nieva, Ph.D. thesis, Universidad Nacional de Cuyo, 1988.
[43] J. G. Sereni, Philos. Mag. **93**, 409 (2013).
[44] A. P. Ramirez, Annu. Rev. Mater. Sci. **24**, 453 (1994).
[45] V. Fritsch, J. D. Thompson, J. L. Sarrao, H.-A. Krug von Nidda, R. M. Eremina, and A. Loidl, Phys. Rev. B **73**, 094413 (2006).
[46] A. S. Edelstein, Phys. Rev. B **37**, 3808 (1988).
[47] H.-U. Desgranges and K. D. Schotte, Phys. Lett. A **91**, 240 (1982).
[48] Q. Si, Physica B **378–380**, 23 (2006).